Advance Sustainable Science, Engineering and Technology

Prediction of $4f^7$-$4f^6 5d^1$ transition energy of Eu^{2+} in oxides based on first-principles calculations and machine learning

Hiroyuki Hori, Shota Takemura, Hayato Obata and Kazuyoshi Ogasawara

School of Science and Technology, Kwansei Gakuin University, 2-1 Gakuen Sanda, Hyogo 669-1337 Japan

dmn11370@kwansei.ac.jp

Abstract. In order to establish a method to predict the $4f^7$-$4f^6 5d^1$ transition energy of Eu^{2+} in oxides, linear regression models were created based on first-principles calculations and machine learning. The model clusters consisting of the central Eu^{2+} and O^{2-} ions closer than the nearest cation were constructed and the $4f^7$-$4f^6 5d^1$ absorption energy of Eu^{2+} in these clusters were calculated by first-principles many-electron calculation using the relativistic discrete variational multi-electron (DVME) method. However, the $4f^7$-$4f^6 5d^1$ absorption energies of Eu^{2+} in oxides calculated by relatively simple first-principles calculations tend to be overestimated by ca. 1.6 eV. In order to improve the accuracy of the prediction, we performed machine learning considering the calculated absorption energy as well as the other electronic and structural parameters as the attributes. As a result, the regression formula to predict the $4f^7$-$4f^6 5d^1$ absorption energy of Eu^{2+} in oxides has been created by machine learning. The $4f^7$-$4f^6 5d^1$ absorption energy predicted by this model are in good agreement with the experimental ones. Therefore, accuracy of the prediction was significantly improved compared to the simple first-principles calculations. In a similar way, a predictive model of the $4f^6 5d^1$-$4f^7$ emission energy of Eu^{2+} in oxides has been also created.

1. Introduction

The $4f^7$-$4f^6 5d^1$ transition energy of Eu^{2+} in oxides are utilized as phosphors for cathode-ray tube, fluorescent lamp, white light emitting diode (WLED) [1]. For theoretical design of novel phosphors based on Eu-doped oxides, it is indispensable to predict $4f^7$-$4f^6 5d^1$ transition energy of fictitious materials. At first, we calculated the $4f^7$-$4f^6 5d^1$ absorption energy by relatively simple first-principles calculations. However, the calculated values tend to be overestimated by ca. 1.6 eV compared to the experimental values. Although the accuracy of the prediction can be improved by performing more sophisticated calculations considering larger model clusters, structural optimization, and so on, such calculations are computationally expensive. Recently, the machine learning technique has been drawing attention as an efficient approach for materials discovery and design [2]. Therefore, we tried to improve the accuracy of the prediction of the $4f^7$-$4f^6 5d^1$ absorption energy by creating a machine learning model considering the calculated $4f^7$-$4f^6 5d^1$ absorption energy as well as the other electronic and structural parameters as the attributes. In this work, in addition to the predictive model of the $4f^7$-$4f^6 5d^1$ absorption energy, the predictive model for the $4f^6 5d^1$-$4f^7$ emission energy was also created.

2. Computational Methods

2.1. First-principles calculation

We performed the first-principles calculations of the $4f^7$-$4f^65d^1$ absorption energy using the relativistic discrete variational multi-electron (DVME) method [3]. We considered 26 oxide crystals and constructed the corresponding model clusters consisting of the doped Eu^{2+} ion and the first-neighbor O^{2-} ions based on the crystal structure data [5-29]. Table 1 shows the oxides and the model clusters considered in this work. The four component relativistic molecular orbitals (MOs) were obtained by performing the MO calculations using the discrete-variational Xα (DV-Xα) method [4]. Then the multiplet energies in the $4f^7$ and $4f^65d^1$ configurations were obtained by performing the configuration interaction (CI) calculations using the relativistic DVME method. The theoretical $4f^7$-$4f^65d^1$ absorption energy was estimated as the energy of the lowest level mainly composed of $4f^65d^1$ configuration relative to the lowest level mainly composed of $4f^7$ configuration.

2.2. Machine learning

We used the machine learning software called WEKA (Waikato Environment for Knowledge Analysis) which was developed in the University of Waikato [30]. For the creation of the predictive model of $4f^7$-$4f^65d^1$ transition energy based on the electronic and structural parameters, the linear regression (single layer perceptron) model was adopted. We considered the following 7 attributes: (1) calculated $4f^7$-$4f^65d^1$ absorption energy, (2) net charge of Eu^{2+}, (3) bond order between Eu and O, (4) barycentre of 5d levels relative to the lowest 4f level, (5) crystal field splitting of 5d levels, (6) average bond length, (7) valence of the substituted cation.

3. Results and discussion

3.1. Predictive model of $4f^7$-$4f^65d^1$ absorption energies

The experimental $4f^7$-$4f^65d^1$ absorption energies in Table 1 [1] were used as the training data for machine learning. Since excessive number of attributes usually results in poor generalization ability, we tried to create a predictive model with as little attributes as possible. By creating predictive models considering the calculated $4f^7$-$4f^65d^1$ absorption energies and two additional parameters as the attributes and comparing the results, we obtained the following predictive model,

$$E = 0.6050E^{calc} - 0.8775Q + 0.7174V - 0.0924, \qquad (1)$$

where E^{calc} is the calculated $4f^7$-$4f^65d^1$ absorption energy, Q the net charge of Eu^{2+}, and V the valence of the substituted cation.

Figure 1 shows the correlation between the $4f^7$-$4f^65d^1$ absorption energies calculated by the simple DVME calculations and the experimental ones. The correlation coefficient was 0.8042 and the calculated values are overestimated by ca. 1.6 eV. Figure 2 shows the correlation between the $4f^7$-$4f^65d^1$ absorption energies predicted by eq. (1) and the experimental ones. The correlation coefficient was 0.9142. Therefore, the accuracy of the prediction of $4f^7$-$4f^65d^1$ absorption energy was significantly improved by net charge of Eu^{2+} and valence of the substituted cation.
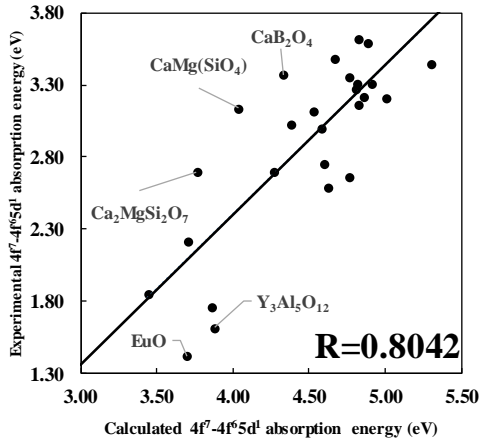
Figure 1. Correlation between the $4f^7$-$4f^6 5d^1$ absorption energies calculated by first-principles calculations and experimental ones.
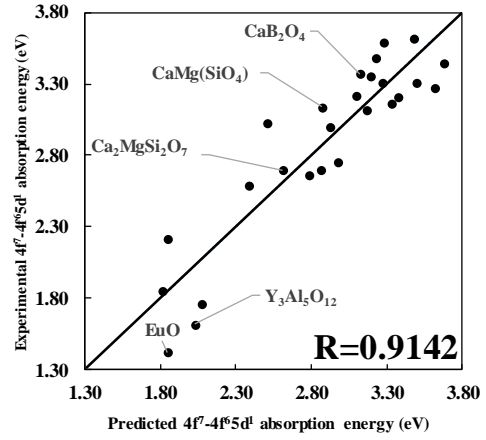
Figure 2. Correlation between the predicted $4f^7$-$4f^6 5d^1$ absorption energies by eq. (1) and experimental ones.

Table 1. Comparison between the $4f^7$-$4f^6 5d^1$ absorption energies predicted by the machine learning model of eq. (1) and experimental ones.

Crystal		Substituted ion	Model cluster	Predicted (eV)	Experimental (eV)	Deference (eV)
$SrSO_4$	[5]	Sr	EuO_{12}^{22-}	3.48	3.62 [1]	-0.14
$CaSO_4$	[6]	Ca	EuO_8^{14-}	3.62	3.27 [1]	0.35
$BaBe_2(BO_3)_2$	[7]	Ba	EuO_{12}^{22-}	3.28	3.60 [1]	-0.32
$KBaPO_4$	[8]	Ba	EuO_9^{16-}	3.38	3.21 [1]	0.16
$KSrPO_4$	[9]	Sr	EuO_9^{16-}	3.34	3.16 [1]	0.18
BaB_8O_{13}	[10]	Ba	EuO_{10}^{18-}	3.68	3.45 [1]	0.23
SrB_4O_7	[11]	Sr	EuO_8^{14-}	3.23	3.48 [1]	-0.25
$Ba_2LiB_5O_{10}$	[12]	Ba	EuO_8^{14-}	3.27	3.31 [1]	-0.04
CaB_2O_4	[13]	Ca	EuO_8^{14-}	3.12	3.37 [1]	-0.25
$Ba_2Mg(BO_3)_2$	[14]	Ba	EuO_9^{16-}	2.93	3.00 [1]	-0.07
$SrAl_2B_2O_7$	[15]	Sr	EuO_6^{10-}	3.17	3.12 [1]	0.05
$CaBPO_5$	[16]	Ca	EuO_{10}^{18-}	3.50	3.31 [1]	0.19
$Ba_2MgSi_2O_7$	[17]	Ba	EuO_8^{14-}	2.98	2.76 [1]	0.22
$Sr_2MgSi_2O_7$	[18]	Sr	EuO_8^{14-}	2.86	2.70 [1]	0.16
$Ca_2MgSi_2O_7$	[19]	Ca	EuO_8^{14-}	2.61	2.70 [1]	-0.09
$BaAl_2(SiO_4)_2$	[20]	Ba	EuO_{12}^{22-}	3.20	3.35 [1]	-0.15
$Li_4Sr_2Ca(SiO_4)_2$	[21]	Ca	EuO_8^{14-}	3.10	3.22 [1]	-0.12
$CaB(OH)(SiO_4)$	[22]	Ca	EuO_8^{14-}	2.51	3.03 [1]	-0.52
$CaMg(SiO_4)$	[23]	Ca	EuO_6^{10-}	2.87	3.14 [1]	-0.27
$EuAlO_3$	[24]	Eu	EuO_{10}^{18-}	2.39	2.95 [1]	-0.56
$Y_3Al_5O_{12}$	[25]	Y	EuO_8^{14-}	2.03	1.62 [1]	0.41
$Lu_3Al_5O_{12}$	[26]	Lu	EuO_8^{14-}	2.08	1.76 [1]	0.32
$BaZrO_3$	[27]	Ba	EuO_6^{10-}	2.78	2.67 [1]	0.11
SrO	[28]	Sr	EuO_6^{10-}	1.85	2.21 [1]	-0.36
EuO	[29]	Eu	EuO_6^{10-}	1.85	1.43 [1]	0.42
CaO	[28]	Ca	EuO_6^{10-}	1.81	1.85 [1]	-0.04

The generalization ability of this model was evaluated by the cross-validation method [30]. The correlation coefficient by the leave-one-out method was 0.8592. Therefore, this model has higher accuracy and reasonable generalization ability.

Table 1 shows the predicted $4f^7$-$4f^65d^1$ absorption energies based on this machine learning model. The difference between the predicted and experimental values are within 0.56 eV, indicating that the absolute values of the $4f^7$-$4f^65d^1$ absorption energies are reasonably predicted.

3.2. Predictive model of $4f^65d^1$-$4f^7$ emission energies
The predictive model of the $4f^65d^1$-$4f^7$ emission energies was also created in a similar way. The experimental $4f^65d^1$-$4f^7$ emission energies in Table 2 [1] were used as the training data for machine learning. We also tried to create a predictive model with as little attributes as possible. By creating predictive models considering the calculated $4f^7$-$4f^65d^1$ absorption energies and one additional parameter as the attributes and comparing the results, we obtained the following predictive model,

$$E = 0.5305E^{calc} - 0.5855Q - 0.7546, \qquad (2)$$

where E^{calc} is the calculated $4f^7$-$4f^65d^1$ absorption energies and Q the net charge of Eu^{2+}.

Figure 3 shows the correlation between the $4f^7$-$4f^65d^1$ absorption energies calculated by the simple DVME calculations and the experimental $4f^65d^1$-$4f^7$ emission energies. The correlation coefficient was 0.8481. Figure 4 shows the correlation between the predicted and experimental $4f^65d^1$-$4f^7$ emission energies. The correlation coefficient was 0.9050 and correlation coefficient of leave one out method was 0.8795. Therefore, this predictive model has higher accuracy and reasonable generalization ability.
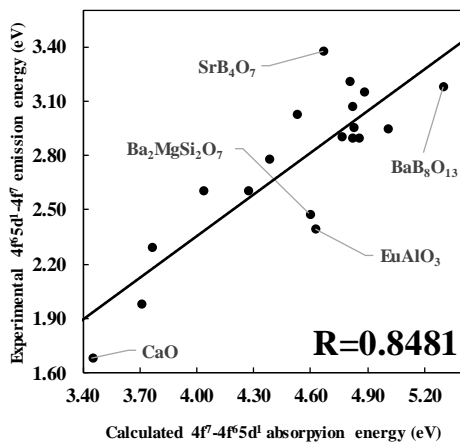
Figure 3. Correlation between the $4f^7$-$4f^65d^1$ absorption energies calculated by first-principles calculations and the experimental $4f^65d^1$-$4f^7$ emission energies.
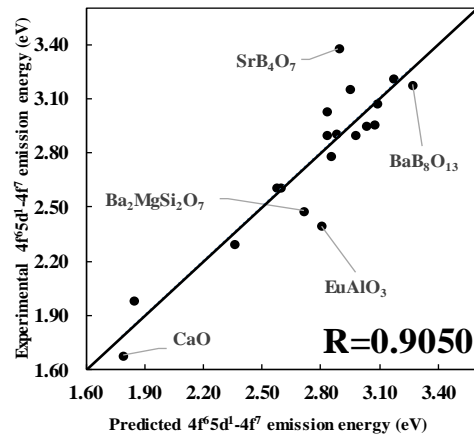
Figure 4. Correlation between the predicted $4f^65d^1$-$4f^7$ emission energies by eq. (2) and experimental ones.

Table 2. Comparison between the $4f^6 5d^1$-$4f^7$ emission energies predicted by the machine learning model of eq. (2) and experimental ones.

Crystal		Substituted ion	Model cluster	Predicted (eV)	Experimental (eV)	Deference (eV)
$SrSO_4$	[5]	Sr	EuO_{12}^{22-}	3.07	2.96 [1]	0.11
$CaSO_4$	[6]	Ca	EuO_8^{14-}	3.17	3.21 [1]	-0.04
$BaBe_2(BO_3)_2$	[7]	Ba	EuO_{12}^{22-}	2.95	3.16 [1]	-0.21
$KBaPO_4$	[8]	Ba	EuO_9^{16-}	3.03	2.95 [1]	0.08
$KSrPO_4$	[9]	Sr	EuO_9^{16-}	2.98	2.90 [1]	0.08
BaB_8O_{13}	[10]	Ba	EuO_{10}^{18-}	3.27	3.18 [1]	0.09
SrB_4O_7	[11]	Sr	EuO_8^{14-}	2.89	3.38 [1]	-0.49
$SrAl_2B2O_7$	[14]	Sr	EuO_6^{10-}	2.83	3.03 [1]	-0.20
$CaBPO_5$	[16]	Ca	EuO_{10}^{18-}	3.09	3.08 [1]	0.01
$Ba_2MgSi_2O_7$	[17]	Ba	EuO_8^{14-}	2.71	2.48 [1]	0.23
$Sr_2MgSi_2O_7$	[18]	Sr	EuO_8^{14-}	2.59	2.61 [1]	-0.02
$Ca_2MgSi_2O_7$	[19]	Ca	EuO_8^{14-}	2.36	3.30 [1]	0.06
$BaAl_2(SiO_4)_2$	[20]	Ba	EuO_{12}^{22-}	2.88	2.90 [1]	-0.02
$Li_4Sr_2Ca(SiO_4)_2$	[21]	Ca	EuO_8^{14-}	2.83	2.90 [1]	-0.07
$CaB(OH)(SiO_4)$	[22]	Ca	EuO_8^{14-}	2.85	2.78 [1]	0.07
$CaMg(SiO_4)$	[23]	Ca	EuO_6^{10-}	2.57	2.61 [1]	-0.04
$EuAlO_3$	[24]	Eu	EuO_{10}^{18-}	2.80	2.39 [1]	0.41
SrO	[28]	Sr	EuO_6^{10-}	1.84	1.98 [1]	-0.14
CaO	[28]	Ca	EuO_6^{10-}	1.79	1.68 [1]	0.11

Table 2 shows the predicted values of the $4f^6 5d^1$-$4f^7$ emission energies based on this machine learning model. The difference between the predicted and experimental values are within 0.49 eV, indicating that the absolute values of the $4f^6 5d^1$-$4f^7$ emission energies are reasonably predicted.

4. Conclusion

By considering the $4f^7$-$4f^6 5d^1$ absorption energy obtained by the first-principles calculation as one of the attributes, we performed machine learning and created the predictive model of the $4f^7$-$4f^6 5d^1$ absorption energy of Eu^{2+} in oxide crystals. As a result, we successfully created the predictive model of the $4f^7$-$4f^6 5d^1$ absorption energy using the calculated $4f^7$-$4f^6 5d^1$ absorption energy, the net charge of Eu^{2+}, and the valence of the substituted cation as the attributes. In a similar way, we also created the predictive model of the $4f^6 5d^1$-$4f^7$ emission energy considering the calculated $4f^7$-$4f^6 5d^1$ absorption energy and the net charge of Eu^{2+} as the attributes. The predicted values are in reasonable agreement with the experimental ones in both models.

References

[1] P. Dorenbos, J. Lumin. **104**, 239 (2003)
[2] T. Lookman, F. Alexander, K. Rajan, Information Science for Materials Discovery and Design (Springer, Switzerland, 2016).
[3] K. Ogasawara, T. Iwata, Y. Koyama, T. Ishii, I. Tanaka and H. Adachi, Phys. Rev. B **64**, 115413 (2001).
[4] A.Rosén, D.E. Ellis, H. Adachi and F.W. Averill, J. Chem. Phys. **65**, 3629 (1976).

[5] S.D. Jacobsen, J.R. Smyth, R.F. Swepe and R.T. Downs, Can. Mineral. **36**, 1053 (1998).

[6] F.C. Hawthorne and R.B. Ferguson, Can. Mineral. **13**, 289 (1975).

[7] Z. Fang, F. Liang, M. Xia, L. Liu, Q. Huang, S. Guo, X. Wang, Z. Lin and C. Chen, Inorg. Chem. **20**, 12090 (2017)

[8] R. Masse and A. Durif, J. Solid state Chem. **71**, 574 (1987).

[9] L. El Ammari, M. El Koumiri, W. Depmeier, K.F. Hesse and B. Elouadi, Eur. J Solid State Inorg. Chem. **34**, 563 (1997).

[10] J. Krogh- Moe and M. Ihara, Acta Crystallogr., Sect. B **25**, 2153 (1969).

[11] J.-B. Kim, K.-S. Lee, I.-H. Suh, J.-H. Lee, J.-R. Park and Y.-H. Shin, Acta Crystallogr., Sect. C **52**, 498 (1996).

[12] Q. Hung, S. Lu, G. Dai and J. Liang, Acta Crystallogr., Sect. C **48**, 1576 (1992).

[13] A. Kirfel, Acta Crystallogr., Sect. B **43**, 333 (1987).

[14] A. Akella and D.A. Keszler, Mater. Res. Bull. **30**, 105 (1995).

[15] F. Lucas, S. Jaulmes, M. Quarton, T. le Mercier, F. Guillen, and C. Fouassier, J. Solid State Chem. **150**, 404 (2000).

[16] R. Kniep, G. Goezel, B. Eisenmann, C. Roehr, M. Asbrand and M. Kizilyalli, Angew Chem. **106**, 791 (1994).

[17] M. Simizu, M. Kimata and I. Iida, Monatsh. chem. **1**, 39 (1995).

[18] M. Ardit, M. Dondi, M. Merlini and G. Cruciani, Phys. Chem. Miner. **39**, 199 (2012).

[19] H. Yang, R.M. Hazen, R.T. Downs and L.W. Finger, Phys. Chem. Miner. **24**, 510 (1997).

[20] A. Kremenovic, P. Norby, R. Dimitrijevic and V. Dondur, Solid State Ionics. **101**, 611 (1997).

[21] A. Akella and D.A. Keszler, Inorg. Chem. **34**, 1308 (1995).

[22] R. Rinaldi, G.D. Gatta and R.J. Angel, Am. Mineral. **95**, 1413 (2010).

[23] Z.D. Sharp, R.M. Hazen and L.W. Finger, Am. Mineral. **72**, 748 (1987).

[24] S. Geller and V.B. Bala, Acta Cryst. **9**, 563 (1956).

[25] A. Nakatsuka, A. Yoshiasa and T. Yamanaka, Acta Crystallogr., Sect. B **55**, 266 (1999).

[26] W. Ahn, Y.J. Kim, Adv. Mater. **8**, 904 (2016).

[27] I. Levin, T.G. Amos, S.M. Bell, L. Faber, T. Vauderah, R.S. Roth and B.H. Toby, J. Solid State chem. **175**, 170 (2003).

[28] M.C. Verbraeken, E. Suard and J.T.S. Irvine, J. Mater. Chem. **19**, 2766 (2009).

[29] G.W. Cunningham, Reactor materials. **6**, 63(1963).

[30] I.H. Witten, E. Frank, M.A. Hall and C.J. Pal, Data Mining: Practical Machine Learning Tools and Techniques (Elsevier, Amsterdam, 2000).